Materials Chemistry and Physics 287 (2022) 126285

Contents lists available at ScienceDirect

Materials Chemistry and Physics

journal homepage: www.elsevier.com/locate/matchemphys

Electrical properties arrays of intersecting of nanowires obtained in the pores of track membranes

I.M. Doludenko **, I.S. Volchkov *, B.A. Turenko, I.O. Koshelev, P.L. Podkur, D.L. Zagorskiy, V.M. Kanevskii

FSRC «Crystallography and Photonics» RAS, Leninskiy Prospekt 59, 119333, Moscow, Russia

HIGHLIGHTS

- The PET track membrane (TM) used for the growth of nanowires was characterized.
- A model for calculating the number of intersections of nanowires was proposed.
- Resistance of an array of $Fe_{0.2}Ni_{0.8}$ nanowires was measured.
- The correlation between the l and the $N_{cros.\ res.}$ with $1/R_{average}$ was established.

GRAPHICAL ABSTRACT

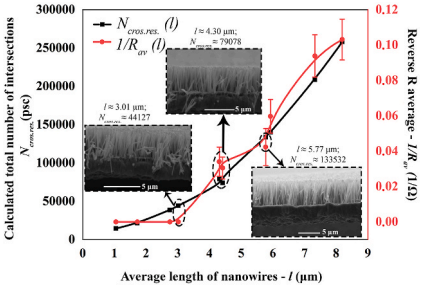

ARTICLE INFO

Keywords:
Fe-Ni alloys
Nanowires
Track polymer membrane
Conductive intersecting nanowire array
Crossing nanowires

ABSTRACT

In the following work by means of matrix synthesis the nanowire arrays of Fe–Ni alloy with elemental composition close to permalloy ($Fe_{0.20}Ni_{0.80}$) were obtained. In capacity of matrix the polyethylene terephthalate (PET) track membranes with angular distribution of pores within the range of ±30° and the diameter of pores in 100 nm were used. As a result, via electrochemical deposition method the metal-polymer composite in the form of nanowire arrays in the polymeric matrix were obtained. The distribution of pores over the surface of track membranes and the average amount of nanowire intersections under a variety of lengths of the grown nanowires were calculated. The resistivity of metal-polymer composite arrays, formed with nanowires of varying length, was measured. The growth boundary conditions and the lengths of nanowire arrays that are essential for obtaining of conducting metal-polymer composite were determined.

1. Introduction

Synthesis of nanostructured materials is one of the most upcoming areas of science nowadays. Such an interest is caused by the enormous potential of possible applications in various directions of science and technology. Metal and semiconductor nanowires/nanorods [1–7] or sandwich-structured with different metal nanoobject, like nanocubes [8–10], can be such promising nanostructured materials. In the case of nanowires and nanorods, their structural features and properties ones depend on the features of the matrix in whose pores growth is carried

* Corresponding author.
** Corresponding author.
E-mail addresses: doludenko.i@yandex.ru (I.M. Doludenko), volch2862@gmail.com (I.S. Volchkov).

https://doi.org/10.1016/j.matchemphys.2022.126285
Received 24 January 2022; Received in revised form 5 May 2022; Accepted 16 May 2022
Available online 18 May 2022

out. In this regard, investigations of the structural features and properties of nanowires of various types, as well as methods for their preparation, are of considerable interest. There is a number of methods for obtaining of nanowires, such as thermal or laser deposition [11,12], which are well suitable for the obtaining of semiconductor nanostructures, and classical methods such as vapor-liquid-solid obtaining [13,14]. Also, a widespread method of obtaining nanostructured materials from metals and alloys is matrix synthesis [15]. The main idea of it is to fill a previously prepared matrix with the required substance. Porous oxide of aluminum (POA) [16,17] and track polymer membranes (TM) [18–20] are the most often to be used as a matrix for synthesis of nanowires with a large aspect ratio. POA matrices are distinguished by a high density of pores with a regular geometric arrangement; however, it is difficult to simultaneously change both the density of pores and their diameter. Also, in POA matrices, there is a certain scatter in the shape of pores, several percent of which are not strictly cylindrical and vertical [21]. Polymer TM are characterized by a chaotic arrangement of pores with the possibility of overlapping one another, however, they differ in flexibility and the ability to purposefully change the shape and diameter of the pores, while the difference in the shape of the pores from each other. In addition, in TM it is possible to vary the density of pores over a wide range, regardless of their diameter and location. A significant difference of TM is the possibility of changing the angle of inclination of the pores to the normal of the polymer film, as well as increasing their density while maintaining the diameter along the entire length.

It is possible to obtain nanostructures of pure metals [22,23] and complex compositions, such as alloys or layered nanowires [24,25] by the matrix synthesis. Thus, nanowires made of Fe–Co, Fe–Ni alloys have magnetic properties depending on the configuration of the received nanowires. These materials are promising for materials for medicine and can also find their application as components of sources and receivers of electromagnetic waves, memristors, elements of flexible microelectronics and others [20,26–30]. In a number of papers, comparison of nanowires from these alloys was made. Thus, in Refs. [27–30] the magnetic properties of nanowires made of alloys obtained by using a POA matrix were investigated and the dependence of the properties on the ratio of elements in the nanostructures, their ordering, and the effect of heat treatment on the structure was shown. The magnetic properties of nanowires depended on the lengths of the synthesized nanostructures.

However, in described works, due to the limitations introduced by the matrix material, it is impossible to properly assess the effect of the degree of pore filling on the physical properties of the obtained arrays of nanowires. It is possible to determine this dependence when using TM as a matrix. Thus, in Refs. [20,31,32], arrays of Fe–Co and Fe–Ni nanowires synthesized in the pores of a polyethylene terephthalate (PET) matrix were studied. Regularities of synthesis were determined for a two-electrode deposition scheme, and the effect of the pore diameter on the orientation of the magnetization vector of nanostructures array and its magnetic properties were shown. However, the use of arrays of nanowires as components of flexible electronics and arrays of sensors or nanoscale circuits [23] requires detailed investigation of the electrical properties of these arrays of nanowires, including the dependence of their electrical properties on the length of nanowires and on the structure of the entire array of nanowires. Thus, the aim of this work was to study the electrical properties of arrays of Fe–Ni alloy nanowires of various lengths in pores with a diameter of 100 nm in a PET matrix, as well as to assess the possibility of controlling the electrical properties of the obtained arrays by changing the nanowire lengths and the configuration of the entire array.

2. Experimental

The arrays of Fe–Ni nanowires of various lengths obtained by electrochemical deposition into the pores of track etched membranes made of PET were studied. The pores in the matrix were through and had a cylindrical shape. The industrial track membranes manufactured by JINR (Dubna, Russia) were used, the parameters of the membranes were as follows: pore diameter (d) – 100 nm; film thickness (h) – 12 μm; pore density (N) – $1.2{\cdot}10^9$ pores/cm^2; angular distribution of pores ±30° along the course of rolling the film (vertically) during irradiation with ions and ±0.5° perpendicular to the course of rolling the film (horizontally) along the course of the scanning ion beam. The process of obtaining of track etched membranes is described in details in Refs. [33, 34].

The preparation of the matrix for the deposition of metal into the pores was made in several stages, shown in Fig. 1. The filling of the pores of the matrix and the production of nanowires were carried out according to the method described in Ref. [35]. The electrodeposition process was carried out in a special galvanic cell. The area of the TM involved in the deposition process was ~1.8 cm^2. The area of the working electrode was 0.17 cm^2 and approximately corresponded to the surface area of the pores of the matrix. A potentiostat/galvanostat "Elins P-2X" was used as a current source. The process was carried out in the potentiostatic mode. The deposition potential was 1.5 V. An iron anode was used for the Fe ions compensation. In Ref. [34], the authors showed that the above-described deposition mode makes it possible to obtain nanowires consisting of an Fe–Ni solid solution based on a Ni lattice with an element ratio of ≈Fe_{24}–Ni_{76}. Arrays of nanowires of different lengths were obtained by changing the time of the electrodeposition process, according to the previously obtained dependence of the average length of nanowires on time, for pores with diameters of 100 nm [36]:

$$l = 4{\cdot}10^{-9}{\cdot}t^3 + 3{\cdot}10^{-5}{\cdot}t^2 + 0.0128{\cdot}t \quad (1)$$

where t – time of electrodeposition, s; l – average nanowire length, μm.

A JSM 6000 PLUS (Jeol, Japan) scanning electron microscope (SEM) was used to control the average length of the deposit arrays of nanowires and to determine the distribution of pores over the surface of TM. The study was carried out in the secondary electron detecting mode at an accelerating voltage of 15 kV.

The electrical characteristics of the nanowire arrays were measured using a resistivity control unit Cresbox (Napson, Japan) using the standard four-probe DC method [37]. The measuring probes were made of tungsten carbide, the distance between adjacent probes was 1 mm, the radius of the tip rounding was ~150 μm, the load on the measuring needle was 50 g. When measuring the electrical characteristics, the contact of each probe with the sample surface was carried out over an area of ≈$0.7{\cdot}10^{-5}$ cm^2. Thus, each probe was in contact not with a single nanowire, but with an array consisting, on average, of 8500 nanowires. The determination of the resulting resistance of the samples under study was carried out at 250 points, evenly distributed over the surface of each sample, in order to obtain averaged values of the resistances of the entire array of nanowires, as well as to level the contribution of the disordered arrangement of pores.

3. Results and discussion

3.1. Matrix characterization

Analysis of the pore distribution over the surface of the PET matrix was carried out to characterize the TM which was used in the work. For this sake, a series of SEM images were made in different parts of the surface of the PET matrix (Fig. 2). The analysis of the pore distribution over the surface was carried out using the single bond method ("nearest neighbor" method) [38–40]. So, the average distance from the center of the pore to the center of the nearest pore was determined by the formula:

$$\bar{r}A = \sum r_i \Big/ n \quad (2)$$

where r_i– distance from the center of a pore to the center of the nearest pore; n – number of pores in the analyzed area.

For the next step, the average value of $\bar{r}A$ was determined over a

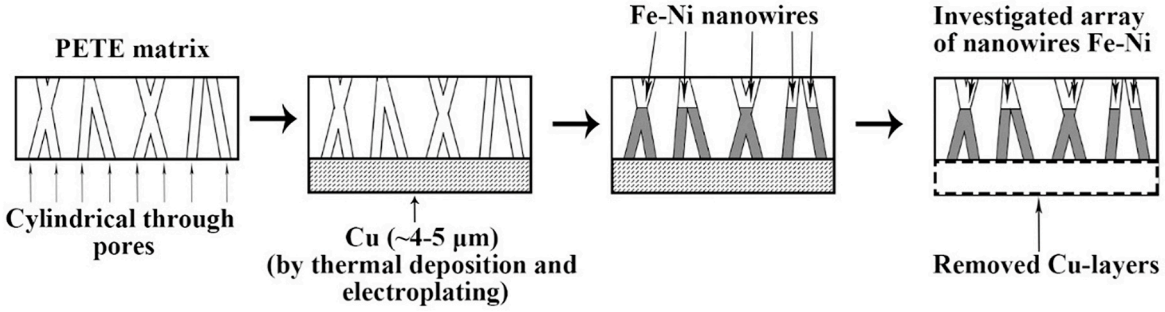

Fig. 1. Stages of the filling of the pores of the matrix and the production of nanowires Fe–Ni in the pores of a PET matrix.

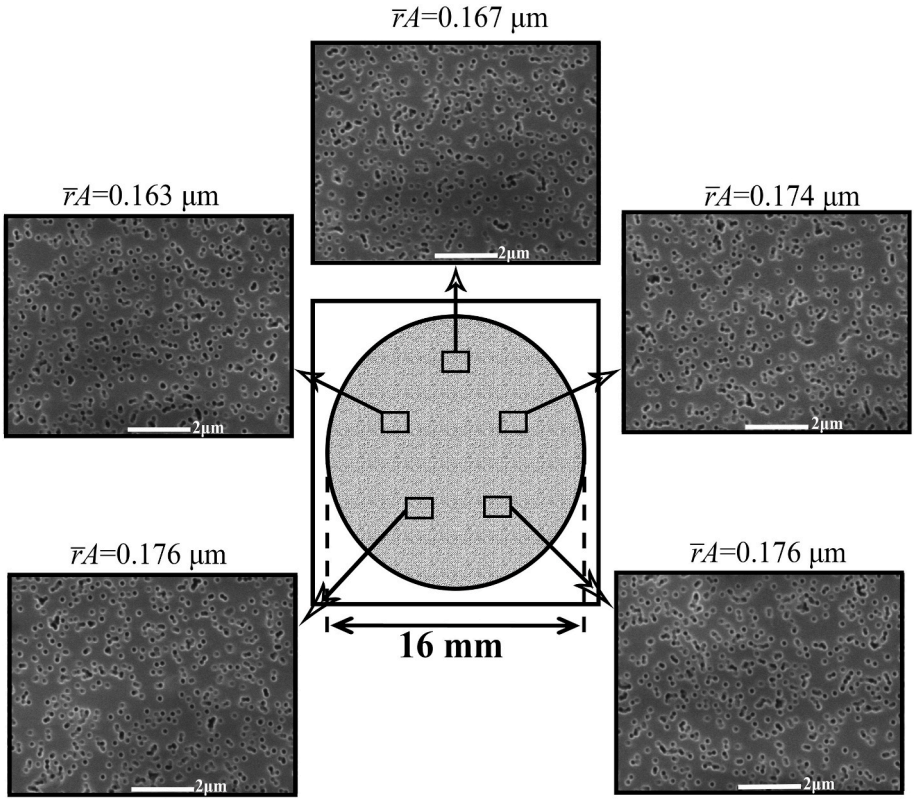

Fig. 2. SEM images of areas on the surface of the PET matrix used to calculate the distribution of pores over the surface.

series of images. To determine the type of pore distribution over the surface of the TM used, the resulting average value, $\bar{r}A = 0.173$ μm, was compared with the average distance to the nearest neighbor characteristic of a random (Poisson) distribution, $\bar{r}E = 0.144$ μm. It was determined by the formula:

$$\bar{r}E = 1\Big/2\sqrt{N} \tag{3}$$

where N – pores density per unit surface (cm^2).

The distribution type was estimated using the Clarke-Evans coefficient (R) [39], according to the formula:

$$R = \bar{r}A/\bar{r}E \tag{4}$$

In our case, R = 1.197, which suggests that the pore distribution on the PET matrix has a deviation from the random (Poisson) distribution, with the presence of group distribution elements. This is clearly seen in the SEM images of the surface of the PET matrix shown in Fig. 2, where there are regions of local pore accumulations. It is also worth noting some uneven distribution of pores over the matrix, characterized by a change in the average distance from the center of the pore to the center of the nearest pore for different regions. This unevenness, most likely, is associated with the peculiarities of the process of obtaining the matrix.

In case of the group type of pore distribution over the surface of the PET matrix, it is necessary to take into account the probability of pore overlap. Overlaps, or partial overlaps, can make a significant contribution to the overall conductivity of the metal-polymer composite, because they are natural areas of formation of an electrical circuit. To take into account partial overlaps of nanowires and estimate their number, it is necessary to enter a condition for accounting for intersections. It is necessary because with a change in the geometric dimensions of nanostructures, a change in the properties of structures is possible, in particular, due to the quantum size effect, which is clearly demonstrated for nanowires made of Bi [41] and Ti [42]. It is worth noting that, although in Refs. [41,42] a change in the properties with a decrease in the nanowires diameter is observed, the nanowires themselves are obtained from a semimetal (Bi) and a superconductor (Ti). In the case of typical metals, which include Fe and Ni, significant changes in electrical characteristics due to the quantum size effect should manifest

themselves only at sizes on the order of interatomic distances. But, it is known that the properties of structures based on FeNi still depend on the sizes larger than interatomic [43,44]. This necessitates the introduction of the conditions for their intersections: since typical metals, as mentioned above, have a pronounced quantum size effect at extremely small sizes, the sizes of the intersection region of two nanowires can be much smaller than the sizes that show a sharp change in properties in Refs. [41,42]. In this case, it is not worth taking into account the cases when the nanowires are only slightly superimposed on each other, because of the possible manifestations of size effects when the sizes of the nanostructured regions formed are too small. In this regard, those pores in which at least 10% of their unit volume overlap will be considered as partially superimposed pores. So, it is necessary to enter the definition of a unit volume ($V_{ind.}$):

$$V_{ind.} = \pi \cdot (d/2)^2 \cdot d \tag{5}$$

where d – pore diameter.

After determining the unit volume, it is necessary to determine the projection of the area of this intersection onto the matrix surface. So, when two pores intersect, the area of their intersection has the shape of an irregular cone, having at the base, in the limiting case, two equal segments. In the case of intersection of pores in the volume, with an angular distribution of pores in the range of ±30° relative to the surface, it can be determined, based on simple geometric calculations, that at least 30% of the pore projection areas are superimposed on the surface (the limiting case when two pores are intersected at angles of 30° and −30°). Now, using the projection of the condition for taking into account the intersections on the matrix surface, it can be determined that superimposed pores will be considered as those pores whose areas of exit to the surface are located within the S_{prob} – the maximum area that satisfies the condition of the limiting partial overlap of pores:

$$S_{prob} = \pi \cdot (1.5 \cdot d - 2 \cdot b)^2 \tag{6}$$

where b – difference between $d/2$ and the altitude of the triangle (k) at the sector formed by the intersection of pores:

$$k = (d \cdot \sin\alpha)/4 \cdot \sin(\alpha/2) \tag{7}$$

where α – angle of a circular arc formed by the intersection of an adjacent pore.

3.2. Determination of pore crossing probability

Next, it is necessary to determine the probability of pore overlap on the matrix surface using the obtained SEM images. Based on the obtained SEM images (Fig. 2) of the regions of the PET matrix, the distance to 4 nearest neighbors for each pore is determined. Then the calculation of the number of pores located within circles of radius $\bar{r}A$, where the center of each circle is the center of each pore participating in the calculation, is carried out. Knowing the number of pores in the image, as well as the distance between the center of each pore and the 4 nearest neighbors, it is possible to calculate the probability of the location of several pores in a circle with radius $\bar{r}A$:

$$P_i = N_i / N_{com} \tag{8}$$

where P_i – the probability of finding the i-th number of pores at a distance $\bar{r}A$ from the center of each pore, N_{com}– total number of pores on the figure, N_i – the number of pores on the figure, at a distance $\bar{r}A$ from which there is the i-th number of pores; i – the number of pores located at a distance $\bar{r}A$ from the center of each pore. Table 1 shows the average values of the probabilities of finding the i-th number of pores in a circle of radius $\bar{r}A$.

Next, it is necessary to calculate the probability of overlap, including partial overlap, according to the previously set condition, on top of each other in the images. To do this, it is necessary to calculate the probability of partial overlap.

Table 1
Distribution of pores over the surface of the PET matrix, as well as the probability of their partial overlap in the subsurface layer characterized by a unit volume.

i (pcs)	1	2	3	4
P_i (%)	100	39.3846	8.123	1.5716
$P_{sup.\ i}$ (%)	–	0.22683	0.009217	0.000499
$N_{sup.\ i}$ (pcs)	–	1622944	17355	99
$P_{i\ lim}$ (%)	100	61.5804	27.7929	6.5395
$P_{sup.\ i\ H}$ (%)	-	0.000932	$1.88699 \cdot 10^{-6}$	$1.16632 \cdot 10^{-8}$
$N_{sup.\ i\ H}$ (pcs)	–	9954	9	0.01

$$P_{\text{sup. } i} = \frac{i!}{\left(\frac{S_{\bar{r}A}}{S_{pore}}\right)^i} \cdot \left(\frac{S_{prob}}{S_{\bar{r}A}}\right)^{i-1} = i! \cdot \frac{{S_{pore}}^i \cdot {S_{prob}}^{i-1}}{{S_{\bar{r}A}}^{2i-1}} \tag{9}$$

where S_{pore} – area of projection onto the surface of one pore; $S_{\bar{r}A}$ – area of a circle with radius $\bar{r}A$; S_{prob} – maximum area satisfying the condition of partial overlapping of pores; $P_{sup.\ i}$ – the probability of superposition of the i-th number of pores in the area of radius $\bar{r}A$.

The average number of pores satisfying the condition of partial overlap was determined by multiplying the total number of pores located on a unit area with (8) and (9):

$$N_{\text{sup. } i} = P_{\text{sup. } i} \cdot P_i \cdot N \tag{10}$$

In this case, it is necessary to take into account the peculiarities of the process of irradiation of a PET matrix by ions for the formation of tracks. So, as mentioned earlier, the pores in the matrices used were located not perpendicular to the plane of the matrix, but at an angle. Moreover, if the horizontal spread of ions was ±30°, then the vertical spread did not exceed ±0.5°. As a result, the resulting pores can form intersections only horizontally, while the vertical displacement of the points of entry and exit of the ion into the PET matrix differed by no more than 0.5 nm at a matrix thickness of 12 μm. In this case, it could not lead to the formation of any significant number of intersections in elevation projection. As a result, when assessing the probability of pore intersections in the volume, it is required to take into account the intersections only in the horizontal projection. The average distance between pores in the horizontal projection will differ significantly from the previously determined average distance to the nearest neighbor $\bar{r}A$. To determine the average distance between the pores in the horizontal projection, one needs to split the obtained SEM images into areas with a height of 100 ± 1 nm and determine the distance between the pores in these areas for all images (example in Fig. 3). Moreover, in the calculation, pores with at least 30% of their area in the analyzed zone will be taken into account as a whole pore. Thus, the analysis of SEM images of a PET matrix (Fig. 2) made it possible to determine the average minimum distance between the pores in the horizontal projection: $\bar{r}H = 0.284$ μm.

After determining $\bar{r}H$, one needs to estimate the probability of pore overlap in bounded regions over the matrix surface. To do this, the steps to determine the probability of finding the i-th number of pores at a distance $\bar{r}A$ from the center of each other (8) should be repeated, however, with some changes in the calculation conditions. So, instead of $\bar{r}A$, the $\bar{r}H$ is used. Also, determination of the distance to 4 nearest neighbors is carried out only within a limited zone. Knowing the number of pores in the images (Fig. 2), as well as the distance between the center of each pore and the 4 nearest neighbors in a limited zone, it is possible to calculate the probability of the location of several pores in a circle with radius $\bar{r}H$:

$$P_{i\ lim} = N_{i\ lim} / N_{com.\ lim.} \tag{11}$$

where $P_{i\ lim}$ – the probability of finding the i pores at a distance $\bar{r}H$ from the center of each pore in limited zone; $N_{com.\ lim.}$ – total number of pores in limited zones; $N_{i\ lim}$– the number of pores on the image in limited

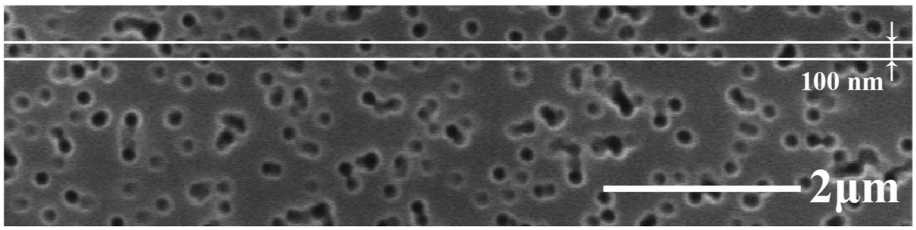

Fig. 3. An example of one region of interest used to calculate the average horizontal pore spacing.

zone, at a distance $\bar{r}H$ from which there is the i pores; i – the number of pores located at a distance $\bar{r}H$ from the center of each pore in a limited zone.

The probability of overlap, including partial overlap, according to the stated condition, on top of each other in bounded areas was determined similarly to (9), however, new conditions were added:

$$P_{\sup.i\ H} = \frac{i!}{\left(\frac{S_{\bar{r}H}}{S_{pore}}\right)^i}\cdot\left(\frac{S_{\bar{r}H\ \lim.}}{S_{\bar{r}H}}\right)^i\cdot\left(\frac{S_{prob}}{S_{\bar{r}H}}\right)^{i-1}\cdot\left(\frac{S_{prob.\ \lim.}}{S_{prob}}\right)^{i-1} = i!\cdot\frac{\left(S_{pore}\cdot S_{\bar{r}H\ \lim.}\right)^i\cdot\left(S_{prob.\ \lim.}\right)^{i-1}}{S_{\bar{r}H}^{3i-1}} \quad (12)$$

where $S_{\bar{r}H\ lim.}$ - area of a circle with radius $\bar{r}H$, in a limited zone; $S_{prob.\ lim.}$ - area of the maximum area that satisfies the condition of partial overlap of pores in a limited zone; $P_{sup.\ i\ H}$ - the probability of superposition of the i pores in an area of radius $\bar{r}H$ in a limited zone.

The average number of pores satisfying the condition of partial overlap in a selected area was determined by multiplying the total number of pores located on a unit area, defined according to the conditions of partial overlap, with (11) and (12), but with the addition of a factor for accounting for pores belonging to two bounded areas (E):

$$N_{sup.\ i\ H} = P_{sup.\ i\ H}\cdot P_{i\ lim}\cdot N\cdot(1+E) \quad (13)$$

The results of the analysis of the pore distribution over the matrix surface are presented in Table 1.

The lengths of the grown nanowires (Fig. 4 (a)) were estimated using SEM. It should be noted that in the case of SEM studies of the lengths of nanowires, the matrix was removed from the samples of arrays of nanowires in a solution of concentrated NaOH (240 g/L) at a temperature of 60 °C.

As it seen in Fig. 4, the grown nanowires have a slope due to the slope of the pores in the PET matrix. Knowing that the angular distribution of pores in the horizontal projection is approximately equal [33,34], as well as knowing the pore density, it is possible to calculate the average number of crossings of pores in the PET matrix per unit volume. For this sake, an assessment of the volume occupied by pores inclined by 0–30° relative to the normal in a PET matrix was carried out:

$$V = \frac{H_f}{\cos\beta}\cdot\left(\pi\cdot\left(\frac{d}{2}\right)^2\right)\cdot\frac{N}{2}\cdot S \quad (14)$$

where V – volume of pores inclined by (0–30)°; H_f – nanowire growth front; β – average angle of inclination of PET matrix pores; S – matrix unit area.

It should be noted, that in the case of calculating the probability of crossing the pores of the matrix it is crucial to take into account the previously advanced condition of partial crossing of nanowires. It is also necessary to take into account that the projection of the deviation of the pores on the surface of the matrix may exceed the average distance between the pores in the horizontal projection. As a result, the nanowire can cross not only with the neighboring nanowire, but also with others, which can lead to double, triple crossings, etc. Taking this into account, the probability of their intersections was calculated, depending on their length:

$$P_{cros.\ i} = \frac{V_{30}}{V_m}\cdot i!\cdot\left(1,8\cdot\frac{V_{-30}}{V_m}\cdot\frac{V_{ind.}}{V_{nanowires}-V_{ind.}}\cdot\frac{\sqrt{\left(l^2-H_f^2\right)}}{\bar{r}H}\right)^{i-1} \quad (15)$$

where $P_{cros.\ i}$ – Probability of crossing nanowires; V_{30}, V_{-30}- the volumes occupied by pores with angle from (0–30)° and (–30-0)°, respectively; V_m – matrix volume; $V_{nanowires} = \pi\cdot(d/2)^2\cdot H_f$– volume of one nanowire; l – average length of nanowires.

Thus, with determined length of nanowire, the probability of their intersection was calculated. The number of intersections was determined:

$$N_{cros.\ i} = P_{cros.\ i}\cdot N \quad (16)$$

where $N_{cros.\ i}$ – the number of intersections of the i-th number of nanowires in the matrix volume.

The results of calculating the number of intersections and partial overlaps in the volume of the matrix are presented in Table 2. It should be noted that although Table 2 shows the calculated amounts of intersections of up to 4 nanowires, it is also possible the intersection of more nanowires, but the probability of this is extremely small, and the

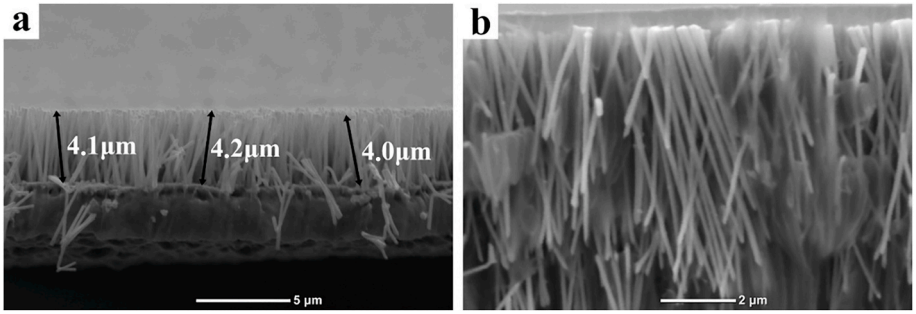

Fig. 4. SEM images of arrays of nanowires: a - an array of nanowires 4.1 μm long; b - a cut of the intersecting array of nanowires. Both the different angle of inclination of the nanowires and the area of intersection are noticeable.

Table 2
Calculation of the number of intersections of up to 4 nanowires satisfying the stated condition for nanostructures of normal length.

l (μm)	$N_{cros.2}$ (pcs)	$N_{cros.3}$ (pcs)	$N_{cros.4}$ (pcs)
8.18	245470	2343	29.83
7.32	196798	1683	19.2
5.92	129167	896	8.3
5.77	122730	830	7.49
4.30	68762	349	2.36
4.14	63761	312	2
3.01	34040	122	0.58
2.75	28546	94	0.41
1.72	11408	24	0.06
1.05	4453	6	0.01

number of such intersections will not have any significant effect on the formation of an electrical circuit.

The total number of intersections and overlaps on the surface was determined as their sum:

$$N_{cros.\ res.} = \sum_{0}^{i} \left(N_{cros.\ i} + N_{sup.\ i\ H}\right) \quad (17)$$

The results of calculating and measuring the resistance are shown in Table 3.

3.3. Electrical resistance of the metal-polymer composites

Resistance for each sample was measured as the average of 250 points equally spaced across the sample area. In the case of growing nanowires to the entire thickness of the matrix, it would be necessary to take into account partial overlaps on the reverse side, but in present case this is not required, since only partial, rather than through, filling of the matrix pores is performed.

Fig. 5 shows the dependence graphs of the total calculated number of intersections $(N_{cros.res.})$ and reverse resistance $(^1/_{R_{av}})$ on the length (l) of nanowires. It can be observed that the dependencies have a similar form, however, there are some deviation regions in dependency of reverse resistivity $(^1/_{R_{av}})$ on the length (l) of the nanowires. The first deviation is observed at nanowire lengths less than 2.7 μm the formation of a continuous conducting chain is not observed, due to the lack of intersections for the formation of a stable electrical circuit, and therefore the resistance of the matrix significantly exceeds hundreds of MΩ. At nanowire lengths longer than ≈2.7 μm, a conducting chain of nanowires begins to form, sufficient enough to measure the resistance, which, with an increase in intersections and nanowire lengths, is characterized by the gradual formation of a continuous stable conducting layer at a nanowire length of ≥4 μm, followed by a relatively smooth conductivity growth, the dependence of which correlates with the dependence of the growth of intersections of nanowires with an increase in their length. The results obtained demonstrate the existence of a critical nanowire length at which, in a given TM configuration, the formation of a continuous conducting array of nanowires is possible.

Table 3
Average resistance, as well as the number of wire crossings in arrays of Fe–Ni nanowires of various lengths.

l (μm)	$N_{cros.\ res.}$ (Pcs)	R_{av} (Ω)
8.18	257808	9.7
7.32	208465	10,66
5.92	140036	16.76
5.77	133532	26.64
4.30	79078	29.4
4.14	74039	32.84
3.01	44127	$0.5{\cdot}10^6$
2.75	38605	$2.7{\cdot}10^6$
1.72	21396	$\gg 10^8$
1.05	14423	$\gg 10^8$

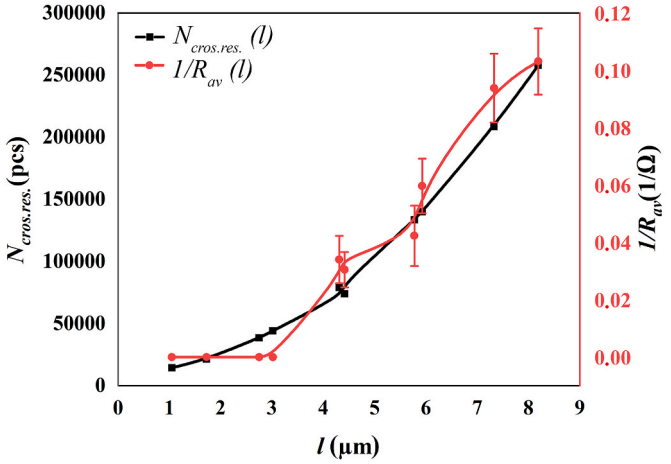

Fig. 5. Dependences of the total calculated number of intersections $(N_{cros.res.})$ and reverse average resistance $(^1/_{R_{av}})$ on the length (l) of nanowires.

Thus, we can summarize that when Fe–Ni nanowires are grown by electrochemical deposition, conductive "chains" of nanowires are formed in PET matrices with inclined pores. In this case, the resistance of an array of nanowires depends on their length and, as a consequence, on the number of intersections. In addition, the correlation of the dependences of the number of crossings on the length $(N_{cros.res.}(l))$ and reverse resistance on the length $(^1/_{R_{av}}(l))$ makes it possible to predict the values of the electrical characteristics of the obtained metal-polymer composites depending on lengths of the grown arrays of nanowires.

Variable values of resistance make it possible to consider these nanostructures as elements of multilayer devices for microelectronics, including flexible ones due to the configuration of the metal-polymer composite array, and also as components of electronic skin.

4. Conclusion

This work shows the possibility of creating a conductive metal-polymer composite based on track membranes with pores filled with Fe–Ni alloy, and obtaining arrays of nanowires with specified electrical properties by establishing the lengths of nanowires and the number of their intersections. The boundary linear dimensions of nanowires forming conducting arrays and the nature of the dependence of the conductivity on the degree of pore filling have been determined. The number of intersections of nanowires is calculated depending on their length and the degree of filling of the matrix. The results of calculations and measurements of resistances coincide: with an increase in the length of nanowires, a decrease in resistance is observed, which indicates the inclusion of a larger number of parallel-connected nanowires into the conducting layer, with an increase in the number of intersections. Insignificant deviations in the monotonic increase in the conductivity of the array with an increase in the length of the nanowires were found. All this makes it possible to obtain elements of microelectronics, magnetic recording, as well as sources and receivers of electromagnetic radiation based on an array of metal-polymer composite obtained by filling TM with metal alloys with specified properties.

CRediT authorship contribution statement

I.M. Doludenko: Conceptualization, Writing – original draft, Visualization, Validation, Writing – review & editing. **I.S. Volchkov:** Conceptualization, Methodology, Formal analysis, Writing – original draft, Writing – review & editing, Visualization, Project administration, Software. **B.A. Turenko:** Investigation. **I.O. Koshelev:** Investigation. **P.**

L. Podkur: Investigation, Writing – original draft. **D.L. Zagorskiy:** Resources, Supervision, Project administration. **V.M. Kanevskii:** Resources, Supervision, Project administration, Funding acquisition.

Declaration of competing interest

The authors declare that they have no known competing financial interests or personal relationships that could have appeared to influence the work reported in this paper.

Acknowledgements

This work was performed using the equipment of the Shared Research Center FSRC "Crystallography and Photonics" RAS and supported by The Ministry of Science and Education of the Russian Federation within the State assignment FSRC « Crystallography and Photonics » RAS.

References

[1] M.U. Farooq, S. Atiq, M. Zahir, M.S. Kiani, S.M. Ramay, B. Zou, J. Zhang, Spin-polarized exciton formation in Co-doped GaN nanowires, Mater. Chem. Phys. 245 (2020), 122756.
[2] H. Xu, H. Shang, C. Wang, Y. Du, Ultrafine Pt-based nanowires for advanced catalysis, Adv. Funct. Mater. 30 (2020), 2000793.
[3] Y. Sun, T. Dong, L. Yu, J. Xu, K. Chen, Planar growth, integration, and applications of semiconducting nanowires, Adv. Mater. 32 (2020), 1903945.
[4] M. Nehra, N. Dilbaghi, G. Marrazza, A. Kaushik, R. Abolhassani, Y.K. Mishra, K. H. Kim, S. Kumar, 1D semiconductor nanowires for energy conversion, harvesting and storage applications, Nano Energy 76 (2020), 104991.
[5] T. Araki, T. Uemura, S. Yoshimoto, A. Takemoto, Y. Noda, S. Izumi, T. Sekitani, Wireless monitoring using a stretchable and transparent sensor sheet containing metal nanowires, Adv. Mater. 32 (2020), 1902684.
[6] T. He, Y. He, H. Li, H. Shi, X. Ma, L. Zhou, F. Zhong, J. Ma, X. Yin, L. Chen, A new choice of electrocatalyst carrier: Ni nanowires induced by magnetic field, Mater. Lett. 293 (2021), 129560.
[7] Z. Wu, H. Zheng, G. Zhang, Y. Deng, Z. Meng, H.U. Wahab, Synthesis of diameter-fluctuating silicon carbide nanowires for excellent microwave absorption, Mater. Chem. Phys. 244 (2020), 122648.
[8] Q. Wang, X. Bai, Y. Zhang, Z. Zhou, M. Guo, J. Zhang, C. Li, C. Wang, S. Chen, Layered assembly of silver nanocubes/polyelectrolyte/fold film as an efficient substrate for surface-enhanced Raman scattering, ACS Appl. Nano Mater. 3 (2020) 1934–1941.
[9] Z. Zhou, X. Bai, P. Li, C. Wang, M. Guo, Y. Zhang, P. Ding, S. Chen, Y. Wu, Q. Wang, Silver nanocubes monolayers as a SERS substrate for quantitative analysis, Chin. Chem. Lett. 32 (2021) 1497–1501.
[10] X. Wang, Y. Wu, X. Wen, X. Bai, Y. Qi, L. Zhang, H. Yang, Z. Yi, Composite structure of Au film/PMMA grating coated with Au nanocubes for SERS substrate, Opt. Mater. 121 (2021), 111536.
[11] M. Tchernycheva, J.C. Harmand, G. Patriarche, L. Travers, G.E. Cirlin, Temperature conditions for GaAs nanowire formation by Au-assisted molecular beam epitaxy, Nanotechnology 17 (2006) 4025.
[12] Y.W. Wang, V. Schmidt, S. Senz, U. Gosele, Epitaxial growth of silicon nanowires using an aluminium catalyst, Nat. Nanotechnol. 1 (2006) 186–189.
[13] V. Schmidt, S. Senz, U. Gosele, Diameter-dependent growth direction of epitaxial silicon nanowires, Nano Lett. 5 (2005) 931–935.
[14] T. Martensson, M. Borgstrom, W. Seifert, B.J. Ohlsson, L. Samuelson, Fabrication of individually seeded nanowire arrays by vapour–liquid–solid growth, Nanotechnology 14 (2003) 1255.
[15] C.R. Martin, Nanomaterials: a Membrane-based synthetic approach, Science 266 (1994) 1961–1966.
[16] Z. Nemati, M.Z. Zamani Kouhpanji, F. Zhou, R. Das, K. Makielski, J. Um, M.-H. Phan, A. Muela, M.L. Fdez-Gubieda, R.R. Franklin, B.J.H. Stadler, J.F. Modiano, J. Alonso, Magnetic isolation of cancer-derived exosomes using Fe/Au magnetic nanowires, ACS Appl. Nano Mater. 3 (2020) 2058–2069.
[17] A.P. Safronov, B.J.H. Stadler, J. Um, M.Z. Zamani Kouhpanji, J. Alonso Masa, A. G. Galyas, G.V. Kurlyandskaya, Polyacrylamide ferrogels with Ni nanowires, Materials 12 (2019) 2582.
[18] O. Picht, S. Muller, I. Alber, M. Rauber, J. Lensch-Falk, D.L. Medlin, R. Neumann, M.E. Toimil-Morales, Tuning the geometrical and crystallographic characteristics of Bi_2Te_3 nanowires by electrodeposition in ion-track membranes, J. Phys. Chem. C 116 (2012) 5367–5375.
[19] A. Pruna, D. Pullini, D.B. Mataix, Influence of deposition potential on structure of ZnO nanowires synthesized in track-etched membranes, J. Electrochem. Soc. 159 (2012) E92.
[20] K.V. Frolov, D.L. Zagorskii, I.S. Lyubutin, M.A. Chuev, I.V. Perunov, S.A. Bedin, A. A. Lomov, V.V. Artemov, S.N. Sulyanov, Magnetic and structural properties of Fe–Co nanowires fabricated by matrix synthesis in the pores of track membranes, JETP Lett. (Engl. Transl.) 105 (2017) 319–326.
[21] D.I. Petukhov, K.S. Napolskii, A.A. Eliseev, Permeability of anodic alumina membranes with branched channels, Nanotechnology 23 (2012) 335601.
[22] S. Kawai, R. Ueda, Magnetic properties of anodic oxide coatings on aluminum containing electrodeposited Co and Co-Ni, J. Electrochem. Soc. 122 (1975) 32–36.
[23] T.R. Kline, M. Tian, J. Wang, A. Sen, M.W.H. Chan, T.E. Mallouk, Template-grown metal nanowires, Inorg. Chem. 45 (2006) 7555–7565.
[24] D.J. Pena, J.K.N. Mbindyo, A.J. Carado, T.E. Mallouk, C.D. Keating, B. Razavi, T. S. Mayer, Template growth of photoconductive metal−CdSe−metal nanowires, J. Phys. Chem. B 106 (2002) 7458–7462.
[25] A.D. Davydov, V.M. Volgin, Template electrodeposition of metals. Review, Russ. J. Electrochem. 52 (2016) 806–831.
[26] O. Dragos, H. Chiriac, N. Lupu, M. Grigoras, I. Tabakovic, Anomalous codeposition of fcc NiFe nanowires with 5–55% Fe and their morphology, crystal structure and magnetic properties, J. Electrochem. Soc. 163 (2016) D83.
[27] J. Alonso, H. Khurshid, V. Sankar, Z. Nemati, M.H. Phan, E. Garayo, J.A. Garsia, H. Srikanth, FeCo nanowires with enhanced heating powers and controllable dimensions for magnetic hyperthermia, J. Appl. Phys. 117 (2015), 17D113.
[28] B. Kalska-Szostko, U. Klekotka, W. Olszewski, D. Satula, Multilayered and alloyed Fe-Co and Fe-Ni nanowires physicochemical studies, J. Magn. Magn Mater. 484 (2019) 67.
[29] A.E. Shumskaya, A.L. Kozlovskiy, M.V. Zdorovets, S.A. Evstigneeva, A. V. Trukhanov, S.V. Trukhanov, D.A. Vinnik, E.Y. Kaniukov, L.V. Panina, Correlation between structural and magnetic properties of FeNi nanotubes with different lengths, J. Alloys Compd. 810 (2019), 151874.
[30] X. Zhang, H. Zhang, T. Wu, Z. Li, Z. Zhang, H. Sun, Comparative study in fabrication and magnetic properties of FeNi alloy nanowires and nanotubes, J. Magn. Magn Mater. 331 (2013) 162–167.
[31] N. Mansouri, N. Benbrahim-Cherief, E. Chainet, F. Charlot, T. Encinas, S. Boudinar, B. Benfedda, L. Hamadou, A. Kadri, Electrodeposition of equiatomic FeNi and FeCo nanowires: structural and magnetic properties, J. Magn. Magn Mater. 493 (2020), 165746.
[32] D.L. Zagorskiy, K.V. Frolov, S.A. Bedin, I.V. Perunov, M.A. Chuev, A.A. Lomov, I. M. Doludenko, Structure and magnetic properties of nanowires of iron group metals produced by matrix synthesis, Phys. Solid State 60 (2018) 2115–2126.
[33] JuTs Oganesjan, S.N. Dmitriev, A.Ju Didyk, V.A. Shchegolev, P.Ju Apel', S. I. Beskrovnyj, Method of Track of Track Membranes Production, RF Inventor's Certificate № 2077938 C1, 1997.
[34] A.V. Mitrofanov, P.Yu Apel, I.V. Blonskaya, O.L. Orelovitch, Diffraction filters based on polyimide and poly (ethylene naphthalate) track membranes, Tech. Phys. 51 (2006) 1229–1234.
[35] I.M. Doludenko, D.L. Zagorskii, K.V. Frolov, I.V. Perunov, M.A. Chuev, V. M. Kanevskii, N.S. Erokhina, S.A. Bedin, Nanowires made of FeNi and FeCo alloys: synthesis, structure, and Mössbauer measurements, Phys. Solid State 62 (2020) 1639–1646.
[36] I Doludenko, Aspects of pore filling in synthesis of FeNi alloy nanowires using track-etched membranes, Inorg. Mater.: Appl. Res. 13 (2) (2022) 531–535, https://doi.org/10.1134/S2075113322020125.
[37] F.M. Smits, Measurement of sheet resistivities with the four-point probe, Bell Syst. Tech. J. 37 (1958) 711–718.
[38] B.S. Duran, P.L. Odell, Cluster Analysis: a Survey, 100, Springer Science & Business Media, 2013.
[39] P.J. Clark, F.C. Evans, Distance to nearest neighbor as a measure of spatial relationships in populations, Ecology 35 (1954) 445–453.
[40] V.N. Gumirova, I.V. Razumovskaya, P. Yu Apel', S.A. Bedin, S.L. Bazhenov, G. S. Abdurashidova, Methods for determining the distribution of pores over the surface of track membranes, Prepodavatel' XXI Vek 2 (2013) 207–213 (in Russian).
[41] E.A. Sedov, K.-P. Riikonen, K.Yu Arutyunov, Quantum size phenomena in single-crystalline bismuth nanostructures, npj Quant. Mater. 2 (2017) 1–4.
[42] J.S. Lehtinen, T. Sajavaara, K.Y. Arutyunov, M.Y. Presnjakov, A.L. Vasiliev, Evidence of quantum phase slip effect in titanium nanowires, Phys. Rev. B 85 (2012), 094508.
[43] A.O. Adeyeye, J.A.C. Bland, C. Daboo, J. Lee, U. Ebels, H. Ahmed, Size dependence of the magnetoresistance in submicron FeNi wires, J. Appl. Phys. 79 (1996) 6120–6122.
[44] Y.J. Zhang, Z.F. Wang, N.L. Wang, G.S. Jiang, W.J. Lu, J. Zhu, Thermal and electrical properties of FeNi/Cu composites, Mater. Sci. Technol. 15 (1999) 1225–1229.